896. Study of railway ground vibrations caused by rail corrugation and wheel flat

J. I. Real[1], A. Galisteo[2], T. Asensio[3], L. Montalbán[4]
Department of Transportation Engineering and Infrastructures, School of Civil Engineering
Technical University of Valencia, 14 Camino de Vera, 46022 Valencia, Spain
E-mail: [1]*jureaher@tra.upv.es*, [2]*algaca@cam.upv.es*, [3]*taasser@cam.upv.es*, [4]*laumondo@cam.upv.es*

(Received 22 August 2012; accepted 4 December 2012)

Abstract. Over the last few years, railway has reached high relevance in cities causing trouble to citizens in form of noise and vibration in the surrounding buildings. Furthermore, these vibrations reach higher values when wheel-rail contact defects appear. The influence that two vibration sources derived from the wheel-rail contact have in their proximity is analyzed in this paper, particularly the defects of rail corrugation and wheel flats. Both defects are examined using the 3D finite element model discussed in a previous paper. The model has been developed and validated with real data and considers a train moving at subsonic speed. The analysis is carried out in the time domain, considering both the quasi-static and dynamic loads and applying dynamic loads to simulate the aforementioned defects. Conclusions are drawn based on the geometric characteristics of the imperfections. Thus, the results of this paper show that, concerning to the wheel flat, an important increase of acceleration peaks near the railway track is observed. Regarding corrugation, it is concluded that the lower corrugation wavelength, the higher vibration amplitude is reached. This work presents a validated method to relate wheel-rail defects to railway vibrations. It may be very useful in identifying the origin of vibrations and to determine which element needs maintenance works.

Keywords: ground vibration, railway track, corrugation, flat wheel, wavelength.

1. Introduction

Ground vibration from railway traffic is generated either by the static axle loads moving along the track or by the dynamic forces which arise in the presence of harmonic or non-harmonic wheel and rail irregularities. The most important frequency range of ground vibration considering human exposure is approximately 5-80 Hz. The excitation by the so called quasi-static axle loads primarily leads to low frequency vibrations. The frequency content of the dynamic excitation is determined by the speed of the vehicle and the wavelength content of the irregularities exciting the wheel-rail contact patch. On a given location, the vibration amplitudes are strongly influenced by the properties of the ground and hence the vibration problem must be seen as an interaction between vehicle, track and ground.

The importance of wheel and rail imperfections is clear when considering the dynamic excitation of ground-borne vibration. In presence of wheel and rail imperfections, the nominal contact forces are disturbed and a dynamic component is introduced into the excitation. In case the contact surface contains a discontinuity, e.g. a wheel flat or rail corrugation, the dynamic excitation is an impulse excitation. The dynamic excitation excites all propagating modes in the ground within the frequency range of the excitation.

Both wheel flat and rail corrugation defects result in an impact excitation on the rail which tends to grow with the size and/or depth of the discontinuity. In references [2-4], measured impact loads excited by wheel flats and long wavelength defects are presented. The results show that load increases with the length of the flatness and the depth of the periodic defect. Furthermore, influence of speed is understood clearly for periodic defects where higher speeds lead to higher forces. However, regarding wheel flats, the speed dependence seems to be more complicated and varies for flats of different size. In [5] measured and simulated contact forces caused by a 100 mm long flatness show that the speed dependence varies with the axle load and

the maximum contact force is excited in the 25-50 km/h speed range. The contact force excited by a long (0.5 m) local defect, on the other hand, shows a simpler speed dependence with a more or less linearly increasing contact load with increasing speed. The more complicated behaviour of the contact force generated by a wheel flat is caused by the potential loss of contact between wheel and rail, which is governed by the size and depth of the flat, the speed and the axle load [6, 7].

Previous studies on wheel-rail contact forces and the influence of wheel and rail defects have primarily focused on damage on rails and wheels and noise. When estimating the influence on ground vibration, the frequency content of the excitation needs to be known and compared with the track and ground response.

2. 3D FE model

A three-dimensional finite element model (FEM) has been developed for the study of ground vibrations caused by wheel-rail defects. The resulting model is based on the geometry and material characteristics of a specific railroad stretch of the tram network in Alicante (Spain), where real data for calibration and validation were measured and registered.

The FEM analysis was performed using ANSYS LAUNCHER software and Rayleigh Damping Theory was considered [1]. Since studied static loads are originated by trains self-weight and dynamic loads from wheel-rail defects, only vertical actions were considered.

The railway structure modelling is determined as a simplification of the real elements placed in the tram section selected for calibration and validation. A detailed view of the 3D model is represented in Figure 1, as a result of it.

In order to dimension the finite element model, a frequency range from 2 to 50 Hz has been set as the limiting parameter. This range includes large part of the frequency which is relevant to the whole internal body perception. Considering elastic vibration theory, the wavelength that restricts the minimum length of the entire model is approximately 50 m. Moreover, the length of elements is lower than 0.5 m. This length was calculated so that 6 nodes were present per wavelength of the Rayleigh waves at the highest frequency [8]. It is also remarkable the fact of using symmetry conditions to avoid the half of the total elements, thus reducing the computational time.

With respect to the sensitivity analysis, calibration and validation, an exposition can be found in [1].

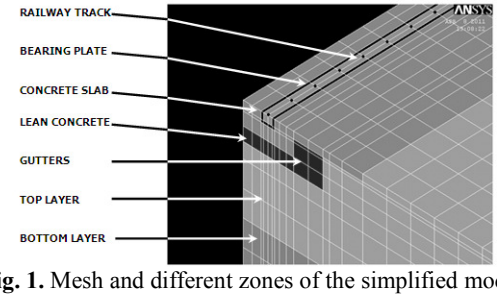

Fig. 1. Mesh and different zones of the simplified model

3. Wheel flat modelling

3.1 Theoretical approach

One of the discrete defects which affects to railway wheels is the presence of wheel flats phenomenon. A wheel flat has its origin in high loads due to wheel-rail contact. These loads are continuously varying their module and position through the wheel path in curves, acceleration

and braking zones or local railway track defects. These circumstances result in a modification of the wheel shape, often resulting in wheel flats, which cause an important increase over the static track loads.

As explained in [9], contact loads reach their maximum at speeds about 20-30 km/h, decreasing at higher speeds up to 100 km/h.

Wheel flats are an important vibration source whose dynamic effects are transmitted far away from the source, since they are a low frequency excitation. In their transmission they cause new problems activating vibration frequencies in the railway track and the soil and producing resonance effects if the new vibration modes match with some characteristic vibration mode of the railway system. The wheel flat frequency depends on the wheel shape and the train speed, as follows in equation (1):

$$f_{pr} = \frac{v}{2\pi r} \tag{1}$$

where v is the train speed and r is the wheel radius.

The wheel movement is assumed to be as shown in Figure 2. The wheel initially rolls around the first corner that contacts the rail, and then the second corner hits the rail, producing overloads.

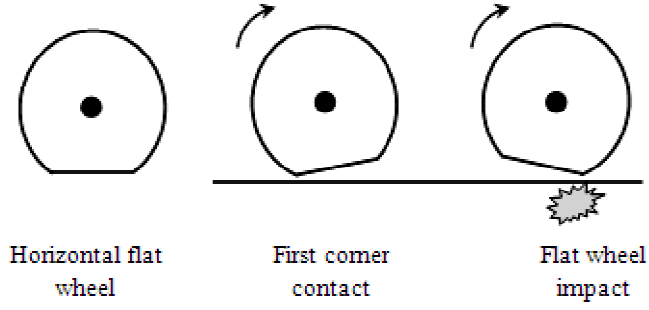

Fig. 2. Flat wheel movement

Another significant parameter is the residence time t_R, which represents the time interval between the appearance of the first corner contact and the wheel flat impact. It is calculated according to equation (2):

$$t_R = \frac{d}{v} \tag{2}$$

where d is the horizontal wheel flat length.

3.2 Estimation of impact strength

Schramm formulation was used to solve the problem, determining the extra dynamic load produced by a wheel flat, commonly used in conventional railway track design. This dynamic overload has the expression shown in equation (3):

$$\Delta\sigma = \frac{15766 + 1.1Q\sqrt{f}}{W} \tag{3}$$

where Q is the load per wheel in N (Q = 45.000 N), f is the flat wheel depth in mm (a common value is f = 2 mm), and W is the resisting moment of the rail in cm^3 (W = 438.22 cm^3). Applying to equation (2) the aforementioned parameters, a dynamic overload of $\Delta\sigma = 1.956 \cdot 10^8$ Pa was obtained.

In order to obtain the transmitted force by the wheel flat, it is necessary to estimate the wheel-rail contact area. It was achieved using the Hertzian contact model, which considers the contact region as a rectangle, calculated as follows.

The transversal size is directly $2b$ = 13 mm.

The longitudinal size is calculated using equation (4):

$$2a = 2 \cdot 1.52 \sqrt{\frac{Qr}{2bE}} \tag{4}$$

where E is the wheel Young's modulus, in this case $E = 2.1 \cdot 10^7$ Pa. It results in a longitudinal dimension of $2a = 9.56 \cdot 10^{-3}$ m.

Hence, the contact area is given by equation (5):

$$S = 2a \cdot 2b = 1.243 \text{ cm}^2 \tag{5}$$

Finally, the total transmitted force per wheel due to the wheel flat is shown in equation (6):

$$F = S\Delta\sigma = 24309 \text{ N} \tag{6}$$

representing about the 50 % of the static self-weight transmitted by the tram (Q = 45.000 N).

3.3 Simulation and results

Before explaining the simulation process, it is important to consider the limitations of the model with regard to the wheel flats. Since loads can only be applied in the nodes of the track model, the phenomenon simulated must present a repetitive behaviour according to the distance between nodes. Specifically in this model, only wheels with a perimeter multiple of 0.5 could be studied.

Two different kinds of forces were modelled. On the one hand, static loads were modelled in every node belonging to the wheel-rail contact region. On the other hand, since a new effect is required to be considered in the model, an impulsive force was introduced simulating the wheel flat defect, according to equation (2). This new force had associated a short application time, considered as 0.001 s, and a module, calculated in the preceding subsection. A 1.50 m wheel perimeter has been supposed, making the dynamic load to actuate every 3 nodes.

The input loads are illustrated in Figure 3, which shows the force transmission diagrams of every node depending on time.

Furthermore, a new frequency appears because of the application of the dynamic force every 3 nodes. The new frequency, considering a tram speed of 30 km/h, is calculated in equation (7):

$$f_{pr} = \frac{v}{2\pi r} = \frac{30/3.6}{1.5} = 5.56 \text{ Hz} \tag{7}$$

This frequency was part of the response registers.

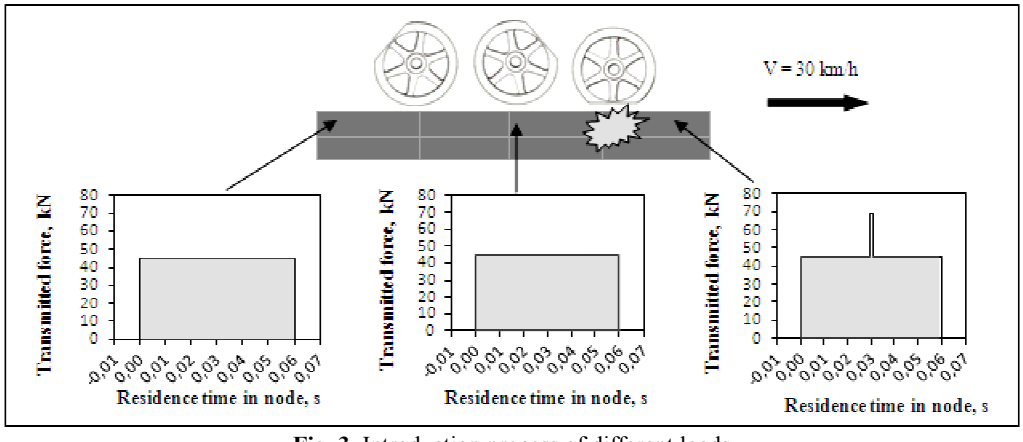

Fig. 3. Introduction process of different loads

The results of the developed model are given in Figure 4, where the model response for two different points is displayed. The locations of the points are 0.3 m from the track in the left graphic case, and 3 m from the track in the right one. Furthermore, the envelopes of the simulation without wheel flat defects are displayed in these graphics, so a comparison between the effects of two different wheel states in ground vibrations may be observed.

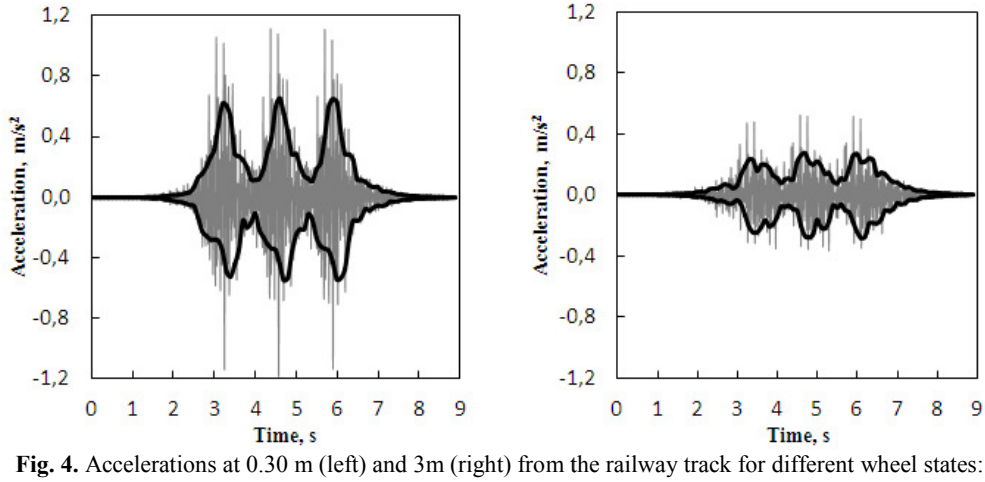

Fig. 4. Accelerations at 0.30 m (left) and 3m (right) from the railway track for different wheel states: wheel flats (gray), wheel without defects (envelope black)

As can be noticed, wheel flats cause an increase in the magnitude response. Furthermore, the attenuation of the ground vibration as the distance from the track increases may be observed.

4. Railway corrugation modelling

4.1 Theoretical approach

Corrugation is a pathology which affects the top of the rail. It is visually identifiable and maintains a relatively constant wave geometry. The wavelength of rail corrugation varies from 25 mm to 1500 mm, but not all the wave lengths can be simulated by the proposed model. Since

every wavelength has to be simulated at least by two consecutive nodes, the minimum wavelength L_m which can be simulated by the model is:

$$L_m = 2d \tag{8}$$

where d is the distance between two consecutive rail nodes.

The model was used to calculate two wavelengths: 1 m and 0.5 m, thus obeying the frequency precision requirement in 2-50 Hz range.

The residence time t_R must be also calculated according to equation (2).

4.2 Dynamic overloads calculation

Since a model that estimates the dynamic overloads because of corrugation is needed, the calculation has been based on an auxiliary quarter car model from [10], as shown in Figure 5.

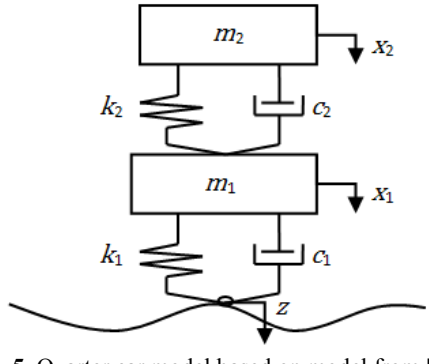

Fig. 5. Quarter car model based on model from [12]

The aforementioned model leads to the following equations of motion:

$$m_2 \ddot{x}_2 + c_2(\dot{x}_2 - \dot{x}_1) + k_2(x_2 - x_1) = 0 \tag{9}$$

$$m_1 \ddot{x}_1 + c_2 \dot{x}_2 + (c_1 + c_2)\dot{x}_1 - k_2 x_2 + (k_1 + k_2)x_1 - c_1 \dot{z} - k_1 z = 0 \tag{10}$$

where m_i, c_i and k_i correspond to the mass, viscous damping and stiffness of each i mass. x_i, $\dot{x}_i$ and $\ddot{x}_i$ correspond to position, velocity and acceleration of each i mass.

The above equations have been solved following indications in [10] with an algorithm implemented in the software Mathematica, whose inputs are the train velocity v, corrugation wavelength L and defects amplitude A. In this way, the railway track is defined as a sinusoidal function.

The values of the parameters used in the model equations are given in Table 1. They correspond to a tram configuration with a concrete mounted track.

Table 1. Parameters for characterization of system mass and vehicle damping

m_1 (kg)	k_1 (N/m)	c_1 (N·s/m)
500	32000000	0
m_2 (kg)	k_2 (N/m)	c_2 (N·s/m)
4000	501745	875

Depending on its corrugation wavelength, two different cases have been analyzed. Their input parameters and dynamic responses are shown in Tables 2-3 and Figures 6-7.

Case 1: 0.5 m element size → $L = 2 \cdot 0.5 = 1$ m.

Case 2: 0.25 m element size → $L = 2 \cdot 0.25 = 0.5$ m.

Table 2. Input parameters for case 1 solving

v (km/h)	L (m)	A (m)
30	1	0.0005

Table 3. Input parameters for case 2 solving

v (km/h)	L (m)	A (m)
30	0.5	0.0005

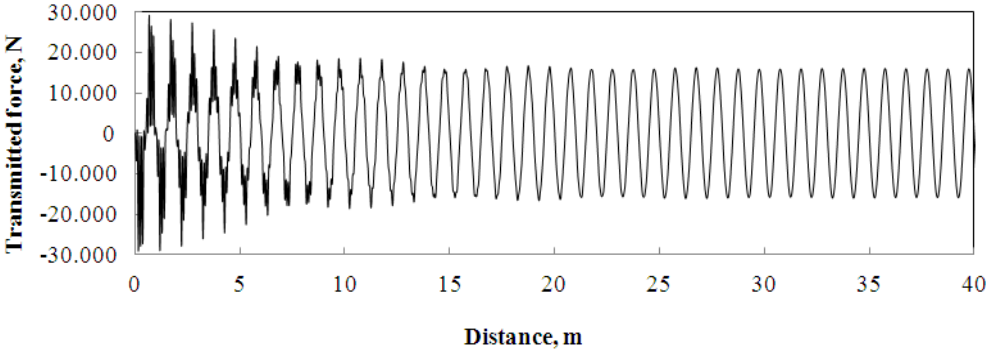

Fig. 6. Transmitted force to the track by a wheel in a track with corrugation defect of 1 m wavelength and $5 \cdot 10^{-4}$ m amplitude

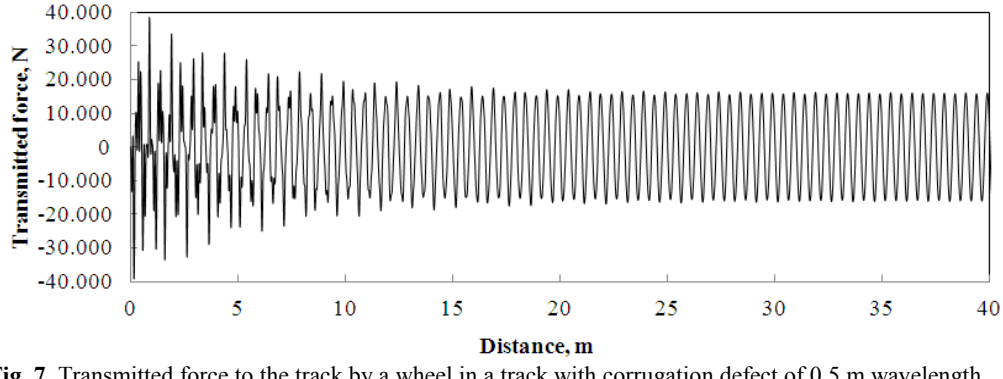

Fig. 7. Transmitted force to the track by a wheel in a track with corrugation defect of 0.5 m wavelength and $5 \cdot 10^{-4}$ m amplitude

4.3 Simulation and results

In the present simulation two simultaneous loads were considered: dynamic loads due to imperfections, which are sinusoidal with a varying wavelength depending on the corrugation and an estimated magnitude of 16 kN, and static loads due to the tram self-weight, which are constant and equal to 45 kN. The superposition of both types of loads is illustrated in Figure 8.

Moreover, a load step distribution was supposed in order to simplify the model. The force applied in every node is considered to be constant, with a value of 29 kN or 61 kN, depending on the node situation as Figure 9 shows, based on superposition of Figure 8.

The following figures show the model responses obtained with the 3D finite element model. The responses were measured in two different points, one of them in the concrete slab (located 0.30 m far from the track) and another one in the soil (located 3 m far from the track).

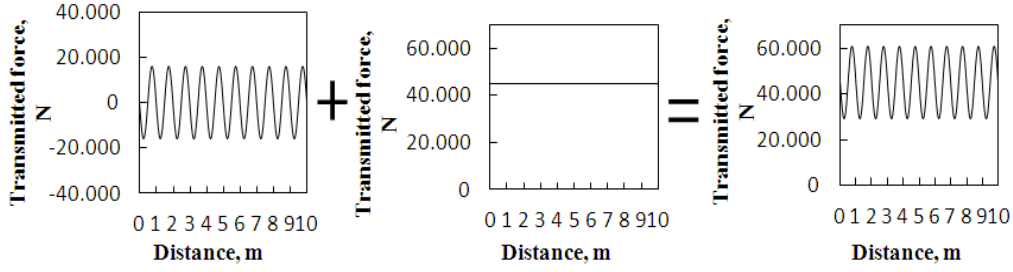

Fig. 8. Superposition of loads transmitted to the track. Dynamic and static loads

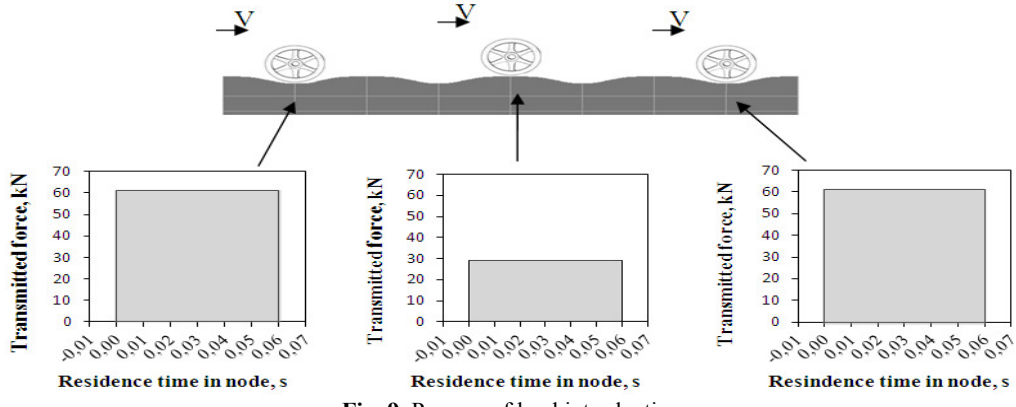

Fig. 9. Process of load introduction

The solution is given for two cases depending on the wavelength of the defects.

Case 1: Wavelength of defects = 1 m.

Case 2: Wavelength of defects = 0.5 m.

As it may be seen in Figures 10-11, higher acceleration values are obtained in the railway track model with imperfections. Furthermore, referring to the frequency of the acceleration peaks obtained, it is higher for lower wavelength defects.

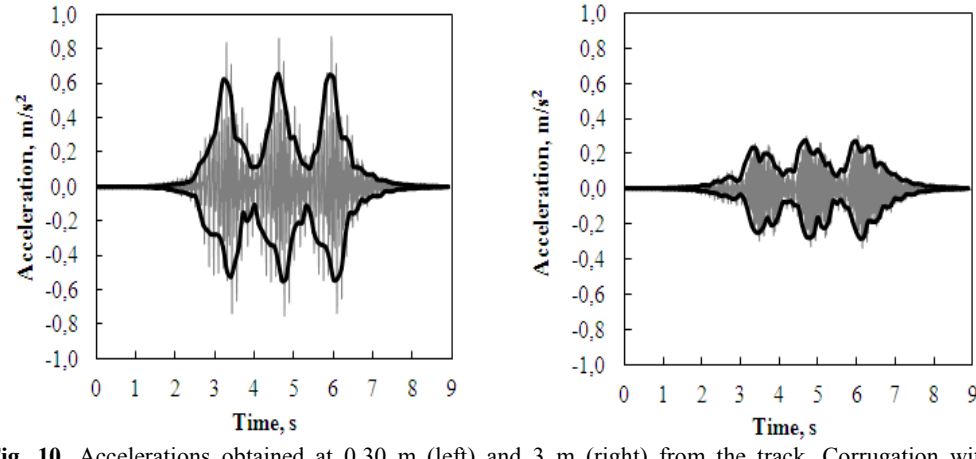

Fig. 10. Accelerations obtained at 0.30 m (left) and 3 m (right) from the track. Corrugation with a wavelength of 1 m and an amplitude of $5 \cdot 10^{-4}$ m (gray) is displayed beside the envelopes of a track in perfect conditions (black)

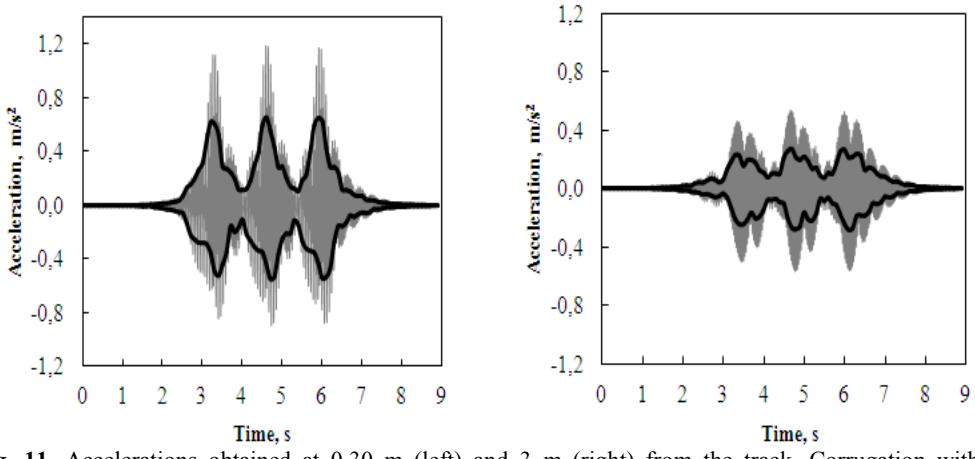

Fig. 11. Accelerations obtained at 0.30 m (left) and 3 m (right) from the track. Corrugation with a wavelength of 0.5 m and an amplitude of $5 \cdot 10^{-4}$ m (gray) is displayed beside the envelopes of a track in perfect conditions (black)

Regarding acceleration values, it has been proved that acceleration peaks are higher when corrugation wavelengths are lower. However, this fact (shown in Figure 12) does not depend on the load values, as these values were the same from the wavelength of the defects.

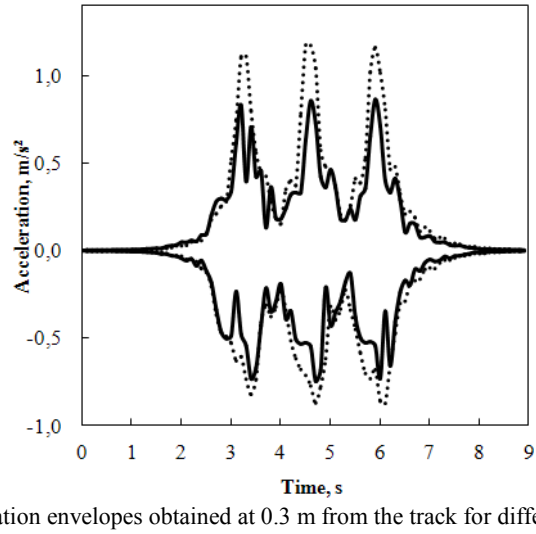

Fig. 12. Acceleration envelopes obtained at 0.3 m from the track for different wavelengths. Wavelength defect = 1 m (continuous line), wavelength defect = 0.5 m (dashed line)

Conclusions

Wheel flats and rail corrugation have been analyzed with the developed finite element model. The results are valid for a frequency range from 2 to 50 Hz. The model considers static loads belonging to the train mass and different dynamics loads produced by both phenomena. From the analysis of the results, the following conclusions can be drawn:

1. The effect caused by wheel flats in railway ground vibrations has been evaluated using Schramm formulation. These defects produce an important increase in the magnitude response, producing high acceleration peaks when the flat wheel impacts on the rail.

2. The effect of rail corrugation in railway vibrations has been taken into account using a quarter car model. The frequency of the acceleration peaks becomes higher when the wavelength of corrugation decreases, since the acceleration peaks are closer.
3. In terms of magnitude, acceleration peaks in a corrugated railway are higher when corrugation wavelengths are lower. It could also be said that the acceleration peak increases with the track frequency of acceleration peaks.

References

[1] **J. I. Real, A. Galisteo, T. Real, C. Zamorano** Study of wave barriers design for the mitigation of railway ground vibrations. Journal of Vibroengineering, Vol. 14, Issue 1, 2012, p. 408-422.
[2] **M. Heckle et al.** Structure-borne sound and vibration from rail traffic. Journal of Sound and Vibration, Vol. 193, Issue 1, 1996, p. 175-184.
[3] **X. Sheng, C. J. C. Jones, D. J. Thompson** A comparison of a theoretical model for quasi-statically and dynamically induced environmental vibration from trains with measurements. Journal of Sound and Vibration, Vol. 267, Issue 3, 2003, p. 621-635.
[4] **L. Auersch** The excitation of ground vibration by rail traffic: theory of vehicle-track-soil interaction and measurements on high-speed lines. Journal of Sound and Vibration, Vol. 284, Issue 1-2, 2005, p. 103-132.
[5] **A. Johansson** Out-of-round railway wheels. Assessment of wheel thread irregularities in train traffic. Journal of Sound and Vibration, Vol. 293, Issues 3-5, 2006, p. 795-806.
[6] **J. C. O. Nielsen, A. Igeland** Vertical dynamic interaction between train and track. Influence of wheel and track imperfections. Journal of Sound and Vibration, Vol. 187, Issue 5, 1995, p. 825-839.
[7] **A. Johansson, J. C. O. Nielsen** Out-of-round railway wheels – wheel-rail contact forces and track response derived from field tests and numerical simulations. Journal of Rail and Rapid Transit, Vol. 217, Issue 2, 2003, p. 135-146.
[8] **Andersen L., Jones C. J. C.** Three-Dimensional Elastodynamic Analysis Using Multiple Boundary Element Domains. ISVR Technical Memorandum, University of Southampton, 2001.
[9] **Hirano M.** Theoretical analysis of variation of wheel load. Railway Technical Research Institute Quarterly Reports, Vol. 13, Issue 1, 1972, p. 42-44.
[10] **M. Melis** Introduction to vertical dynamics of railway tracks and to digital signals in trains. School of Civil Engineering, Madrid, Spain, 2008.